scientific reports

Check for updates

OPEN

Detection of IDH mutation in glioma by desorption electrospray ionization (DESI) tandem mass spectrometry

Mahdiyeh Shahi[1], Steven Pringle[2], Michael Morris[2], Diogo Moniz Garcia[3], Alfredo Quiñones-Hinojosa[3] & R. Graham Cooks[1]✉

Desorption electrospray ionization (DESI) tandem mass spectrometry (MS) is used to assess mutation status of isocitrate dehydrogenase (IDH) in human gliomas. Due to the diffuse nature of gliomas, total gross resection is not normally achieved during surgery, leading to tumor recurrence. The mutation status of IDH has clinical significance due to better prognosis in IDH-mutant patients. The mutant IDH converts alpha-ketoglutaric acid (α-KG) into 2-hydroxyglutarate (2HG), which accumulates abnormally in cells. Immunohistochemical staining (IHC) and genetic testing, the gold standards, are incompatible with intraoperative applications but DESI tandem mass spectrometry (MS/MS) can be used to assess the mutation status of IDH enzyme from tissue intraoperatively. Here, on off-line evaluation is made of the performance of two different types of mass spectrometers in characterization of IDH mutation status. The intensity of 2HG is measured against glutamate (Glu), an intrinsic reference molecule, in both tandem MS measurements. In both cases using DESI clear separation between IDH-mutant (mut) and IDH-wildtype (wt) samples ($p < 0.0001$) is observed, despite the short analysis time. Due to the higher detection sensitivity, multiple reaction monitoring experiments using a triple quadrupole show slightly better performance compared to product ion MS/MS performed on a simple linear ion trap. Both DESI-MS platforms are capable of providing information on IDH mutation status, which might in future be used at the time of surgery to support decision-making on resection regions, especially at tumor margins.

Keywords Multiple reaction monitoring (MRM), 2-hydroxyglutarate, Oncometabolite, Molecular diagnostics, Brain cancer, Ambient ionization

Gliomas are the most common primary malignant brain tumors that arise in the central nervous system (CNS). They are classified into different subtypes, including isocitrate dehydrogenase (IDH) mutant (mut) and wildtype (wt)[1]. Given the heterogeneity of the gliomas, current diagnosis guidelines rely increasingly on molecular features. The 2021 World Health Organization (WHO) classification of CNS tumors now includes the mutation status of IDH as a molecular marker to differentiate between IDH-mut astrocytomas and glioblastomas (GBMs)[1]. This feature has been recognized as an important diagnostic marker due to its prognostic significance and the higher overall survival rates for patients with IDH-mut gliomas, and this can affect treatment approaches as new medications targeting IDH-mut gliomas are currently in clinical trials[2–4]. The primary treatment for glioma is craniotomy surgery. However, with the diffuse nature of gliomas, a clear distinction between the infiltrated and paracancerous tissue remains challenging within the current standard of care. Rapid and accurate assessment of tumor margins could assist surgeons in decision-making at the time of resection, achieving optimal tumor removal while minimizing surgical deficits[5–7].

The heterozygous mutations in the IDH enzymes, which have an important role in the Krebs cycle, introduce a neomorphic activity where the mutant dimer converts alpha-ketoglutaric acid (α-KG) into 2-hydroxyglutarate (2HG)[8] as shown in Fig. 1 A. Abnormal accumulation of 2HG in glioma tissues (up to 30 mM in the cytoplasm) has been found to be an indication of IDH mutation[9–11], while 2HG remains at trace concentrations in non-infiltrated tissues. Intraoperative detection of IDH mutation could affect the extent of tumor resection and

[1]Department of Chemistry, Purdue University, West Lafayette, IN 47907, USA. [2]Waters Corporation, Stamford Ave, Wilmslow SK9 4AX, UK. [3]Department of Neurosurgery, Mayo Clinic, Jacksonville, FL 32224, USA. ✉email: cooks@purdue.edu

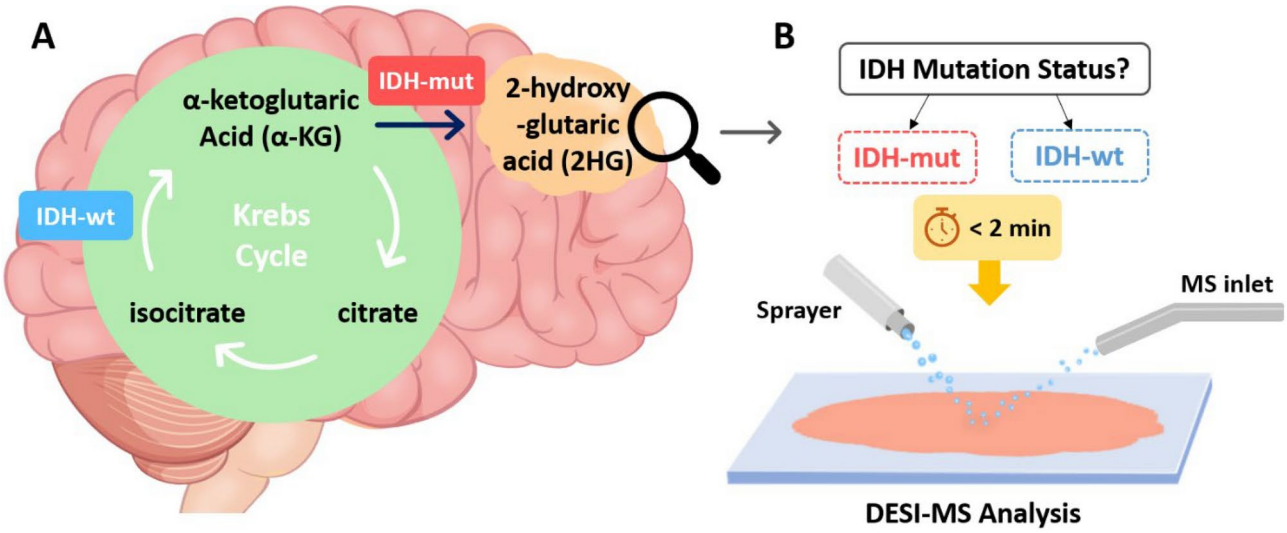

Fig. 1. **A** Mutation in IDH introduces a distinct metabolic pathway where α-KG is reduced to 2HG in an NADPH-dependent manner. **B** DESI-MS enables rapid analysis of unmodified brain smears to evaluate the mutation status of IDH enzyme.

treatment protocols at the time of surgery, thereby improving patient outcomes. Notably, the infiltrated tumor cells that remain beyond the surgical margins often cause the tumor to recur and, in some cases, to progress to higher-grade gliomas[12]. Despite the diagnostic and prognostic significance of IDH mutation, intraoperative identification of IDH mutation at the molecular level remains unmet, with postoperative use of current standard methods of immunohistochemical staining (IHC) and genetic testing[13,14]. Microscopic evaluation of the tissue slides, the most common intraoperative diagnostic method, only provides morphological features of the infiltrated tissues and lacks molecular information[13,14].

The need to delineate between the tumor and the adjacent non-infiltrated tissues has led to the development of various diagnostics for preoperative and intraoperative applications. Magnetic resonance imaging (MRI) and computed tomography (CT) are routinely used for tumor navigation and to assess the extent of resection, with the former providing limited information on molecular features[15,16]. However, insufficient analytical sensitivity and brain shifting are common in MRI which can influence the precision and accuracy of location assessments[17]. Magnetic resonance spectroscopy (MRS), optical coherence tomography (OCT), fluorescence spectroscopy, infrared (IR) spectroscopy, and Raman spectroscopy have been explored for intraoperative applications given their potential for providing molecular information based on chemical bonding[9,18–20]. Mass spectrometry (MS) is a sensitive and rapid analytical tool that directly detects molecules in complex matrices[21]. Integration of MS with chromatographic techniques or utilization of tandem MS enables analysis of complex samples like brain tissue[22,23]. The inherently slow nature of chromatography and time-consuming sample preparation steps inhibit the use of LC–MS for intraoperative applications where time is of the essence. Several ambient ionization methods have been developed and used as intraoperative diagnostic tools with minimum to no sample preparation requirement[24]. Rapid evaporative ionization mass spectrometry (REIMS)[25], MasSpec Pen[21,26], picosecond infrared laser mass spectrometry (PIRL-MS)[27], SpiderMass[28], and desorption electrospray ionization (DESI) have all been used for tumor analysis[22]. In DESI-MS, a high voltage (typically 4–5 kV) and pneumatic force is used to ionize and nebulize a solvent and the resulting charged microdroplets are propelled onto the surface of the sample where extraction and desorption of analyte molecules occurs. This produces a stream of secondary droplets containing ionized molecules that enter the mass spectrometer[29,30]. DESI has been used for the analysis of a variety of tissues in both imaging and smear diagnosis, in some cases using high-throughput tissue arrays and MS/MS experiments[11,31–34].MS/MS selectively records fragment ions to enhance measurement specificity and minimize isobaric and isomeric interferences. Product-ion spectra record a mass range of interest to detect fragment ions coming from mass-selected precursor ions undergoing collision-induced dissociation (CID)[35]. Multiple reaction monitoring (MRM) is a form of tandem MS usually done using triple quadrupole (TQ) mass spectrometers. Here the first quadrupole selects ions of a particular mass, the second allows their CID and the third records product ion mass and intensity[36,37]. In MRM, selection of appropriate product ions is essential to achieve molecular specificity. Thus, before performing MRM, product ion spectra of analytes of interests are recorded to identify reliable diagnostic fragment ions. TQs and linear ion traps (LIT) are mass analyzers that can be used for tandem MS, although the former is limited to two stage MS/MS while the later enables MS^n experiments. On the other hand, performing two stage MS/MS using TQs benefits from higher analytical sensitivity (lower detection limit) and faster scanning rates compared to LITs. The combination of ambient ionization and tandem mass spectrometry in the form of DESI-MS/MS enables rapid and specific detection of small biomarkers in complex samples like brain tissue with minimum sample preparation, which hold promise as an intraoperative diagnostic tool (Fig. 1B).

Here, DESI was coupled to a TQ and a LIT in separate experiments to perform tandem MS on brain smears to detect the presence of IDH mutations in glioma biopsies. A total of 64 individual human glioma smears were analyzed using product ion MS/MS with an LIT and, separately, also by MRM performed using a TQ. Methodology for the detection of IDH mutation in glioma was reported in previous studies[10,11,22,38,39]. The intensity of 2HG was measured against Glu to assess IDH mutation status and to correlate tumor infiltration in margins to the 2HG concentrations. The robustness of this ratiometric method was examined here by performing offline experiments using two different mass spectrometers and tandem MS experiments. Performance of DESI-product ion MS/MS and DESI-MRM for diagnosis of IDH mutation was assessed and compared to data from a previously reported intraoperative study[22].

Results

For this study, 64 glioma biopsies, including 38 tumor cores and 26 margins, were analyzed. See Supplementary Table S1 and S2 for clinical information, biopsy locations, and IDH mutation scores. Figure 2 shows typical mass spectra and TIC bar plots of IDH-mut and IDH-wt gliomas. Activation by CID of deprotonated 2HG (*m/z* 147) and Glu (*m/z* 146) induces dehydration, producing fragment ions with a neutral loss of 18 (*m/z* 129 and *m/z* 128, respectively). Due to the neomorphic metabolic aberration, IDH-mut samples have significantly higher 2HG/Glu ratio, than that observed in IDH-wt gliomas.

The average IDH mutation score of the three experiments was calculated to evaluate and compare the performance of the product ion MS/MS and MRM methods. It should be noted that for DESI-MS prediction of IDH mutation status, only core biopsies (n = 38) were included. The area under the curve (AUC) of the ROC curves (Fig. 3 A and D) is 0.99 and 0.99 for the product ion MS/MS and MRM-profiling, respectively. From the ROC curve analysis, the estimated optimal cutoff using the Youden index with highest sensitivity and specificity was 0.35 for the DESI-product ion MS/MS; however, it is possible to avoid false positives by using a higher value, 0.73, as the optimized threshold for IDH mutation discrimination. The cutoff for MRM-profiling using the Youden index was 0.76 and this gave no false positives. These values are close to the obtained threshold (0.83) from an intraoperative study[22], for more details see Supporting statement S2. Figure 3 B and E show clear separation of IDH-mut and IDH-wt in the box plots with median line and whisker at ± 1.5 IQR. When performing the Wilcoxon rank-sum test, the IDH-mut and IDH-wt groups were found to be statistically

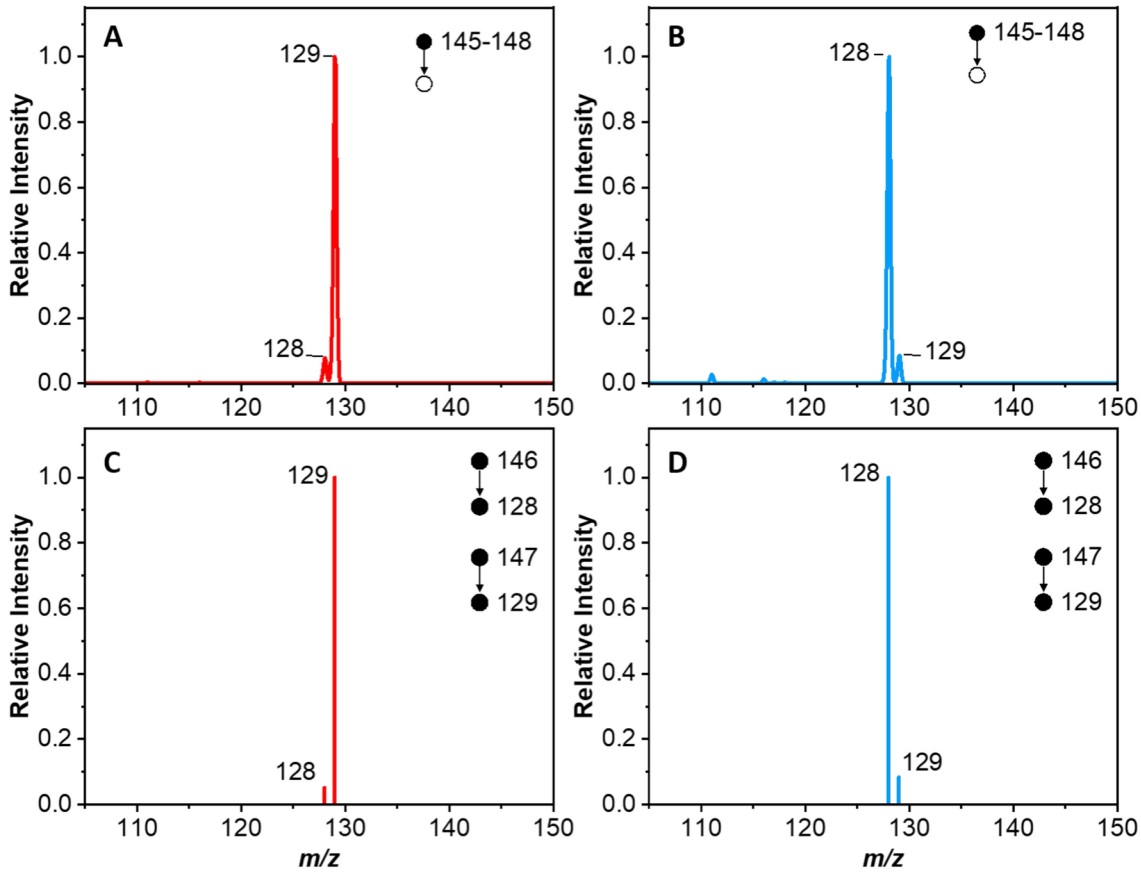

Fig. 2. **A and B** Representative spectra of an IDH-mut and an IDH-wt glioma samples obtained through MS/MS measurements measured using the LIT. **C and D** MRM (TIC) channel intensity plots of the same smears measured using the TQ. All measurements were performed in negative mode. (In C and D only data for the two MRM transitions was collected).

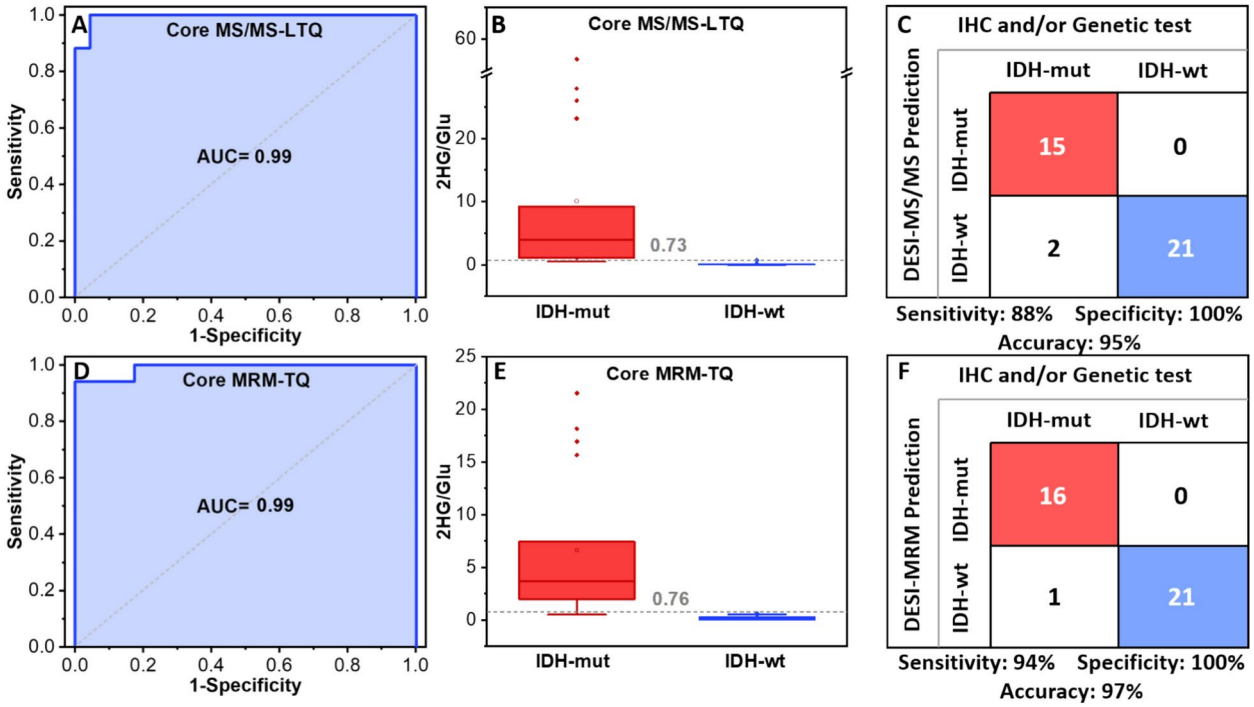

Fig. 3. **A and D** ROC curve plots of the IDH mutation scores for product ion MS/MS and MRM experiments. **B and E** Box and whisker plots of IDH mutation scores for IDH-mut and IDH-wt gliomas obtained with MS/MS and MRM ($p < 0.0001$). **C and F** Confusion matrix comparing the DESI-product ion MS/MS and DESI-MRM predictions to the clinical diagnosis, with the corresponding sensitivities, specificities, and accuracies. These results are for 38 core biopsies.

significant with $p < 0.0001$. Sensitivity, specificity, and accuracy from core biopsies were 88%, 100%, and 95%, respectively, using DESI-product ion MS/MS (Fig. 3 C) and 94% sensitivity, 100% specificity, and 97% accuracy for the MRM technique, as shown in Fig. 3. F. MRM measurements showed better performance due to a higher analytical method sensitivity (lower detection limit).

High concentrations of 2HG (above the cutoff values) were observed in 67% of margin biopsies from IDH-mut patients, which indicates that IDH-mutant tumor cells infiltrate beyond the surgical margins (n = 26). When comparing the results of this study to the intraoperative MS data[22], product ion MS/MS assessments showed 94% agreement, and 96% of MRM predictions agreed with the intraoperative assessments. These deviations from 100% are assumed to be due to the heterogeneity of the tumors and smear storing conditions. It should be noted that each individual smear was analyzed six times in total.

Discussion

Despite using different DESI sources and two different types of mass spectrometers, similar performance was obtained and consistent conclusions were reached. The DESI sources allowed analysis of unmodified brain smears while tandem MS analysis minimized isobaric and isomeric interferences. Detection of high concentrations of 2HG as a unique biomarker of IDH-mut gliomas provides information on the mutation status of IDH, with data acquisition and interpretation times of less than two minutes. The assessment of the IDH mutation status with product-ion scanning MS/MS and MRM provided clear separation between IDH-mut and IDH-wt core biopsies. DESI-MRM experiments showed higher clinical sensitivity due to lower instrumental detection limits and the higher ion currents available with the new generation DESI ion source. These results, together with previous reports, show the robustness of the ratiometric method for detection of IDH mutation in glioma samples. In addition, the close proximity in mass of ionized 2HG and Glu facilitates prediction of mutation status without complicated data processing.It should be noted that the brain smears studied had undergone several freeze–thaw cycles and had been analyzed several times; this might have affected their quality; however, both tandem MS experiments showed agreement with the clinical results. A majority of the margin biopsies displayed high 2HG/Glu ratios which are attributed to the tumor infiltration beyond the surgical margins. The speed of the method, its high analytical sensitivity, and minimal requirements for sample preparation make DESI-MS a promising diagnostic tool for intraoperative application. Knowledge of IDH mutation status can guide the extent of resection and personalize treatment strategies.

Conclusion

Similar workflows with two different mass spectrometers were used to predict the mutation status of IDH in human glioma specimens. Unmodified glioma smears were analyzed by DESI tandem MS, with predictions

available in less than two minutes. The speed and accuracy of the measurements allow for the intraoperative diagnosis of the presence of IDH mutation in glioma at the molecular level. DESI requires minimal tissue preparation, while the use of tandem mass spectrometry attenuates interferences from matrix components including isobars and isomers. Clear separation between IDH-mut and IDH-wt gliomas with a strong correlation of high ratio of 2HG/Glu in IDH-mut glioma was observed ($p < 0.0001$). 2HG accumulation was detected in 67% of margin biopsies, indicating that tumor infiltration extends beyond the resection cavity. DESI-product ion MS/MS and DESI-MRM experiments showed similar performance with slightly better sensitivity being observed in the MRM results, as expected. For product ion MS/MS experiments, sensitivity, specificity, and accuracy of 88%, 100%, and 95% were obtained, respectively, while MRM measurements had 94% sensitivity, 100% specificity, and 97% accuracy. Moreover, comparing the product ion MS/MS and DESI-MRM methods for predicting IDH mutation status in all biopsies shows 94% and 96% agreement, respectively, with previously published intraoperative MS assessments[22] run on resected glioma tissue from the same patient. The small number of incorrect MS predictions can be attributed to the freezing–thawing artifacts, tissue degradation over time, and sample storing conditions, this highlights the value of intraoperative assessments which showed 100% agreement for core biopsies with independent immunohistochemical or genetic testing data. DESI-tandem MS can detect IDH mutation from core biopsies and for margin biopsies it provides information on tumor infiltration to assist surgeon decision-making on the extent of tumor resection. This is achieved on a timescale suitable for deployment intraoperatively.

Materials and methods

Brain samples

This study used a set of 64 unmodified fresh-frozen glioma biopsies provided to Purdue University by Mayo Clinic, Fl, for offline analysis of samples associated with a previous intraoperative study[22] according to a material transfer agreement between the two institutions. The research was conducted in accordance with the Mayo Clinic Jacksonville, Institutional Review Board (IRB) approval (IRB #19–010,725, protocol title: *Advanced Development of Desorption Electrospray Ionization Mass Spectrometry for Intraoperative Molecular Diagnosis of Brain Cancer Using Pathology Biopsies*) and relevant guidelines and regulations. All patients involved in this study provided written informed consent. For each patient, multiple biopsies were collected, processed, and transferred from Mayo Clinic as previously reported[40]. After the frozen tissues had been thawed, small amounts of the specimens (approximately 5–10 mg) were smeared onto microscope glass slides using a 3D-printed smearing tool[41] and subjected to DESI-MS/MS examination. When the size of the biopsies allowed, a portion was sent to Purdue for this study.

Clinical diagnosis

During surgeries, biopsies from multiple locations (tumor core and margin) were collected, a number of them were provided to the attending MS researcher, and the remaining sections were sent to the pathology lab for clinical diagnosis. Brain smears analyzed intraoperatively by MS were also sent to the pathology lab for hematoxylin and eosin (H&E) staining for further evaluation, including diagnosis (i.e., glioma, normal brain, blood, and necrosis), smear quality, and estimated tumor cell percentage (TCP). Biopsy locations (e.g., core or margin with respect to MRI of tumor) were determined using a neuronavigation system, with corresponding snapshots recorded. Immunohistochemical (IHC) staining and/or polymerase chain reaction (PCR) sequencing were performed on core biopsies to determine the IDH genotype for each patient, as previously reported[22]. When the size of the left-over biopsies allowed, they were frozen and sent to Purdue University for additional analysis.

MS examination

MS assessment of the IDH mutation status of each biopsy was performed by recording product ion MS/MS scans using an LIT (Thermo LTQ) and MRM-profiling using a TQ (Xevo™ TQ-S micro mass spectrometer, Waters) operated in negative ion mode. A homebuilt DESI source and a prototype DESI (Waters) were coupled to the LIT and TQ, respectively. The movement of the samples was performed using an automated moving stage. It should be noted that this study was focused on smear diagnosis rather than spatial mass spectrometry (MS). The Waters prototype source gave much higher ion currents (see Table S3).

For DESI analysis using the LIT, a solvent mixture of DMF-ACN-EtOH (25:37:38) introduced at 2 uL/min into the sprayer at held at 4.5kVcreating the charged microdroplets used for the extraction and ionization of biomarkers from the smeared samples. Once the angle and distance from the sample to the mass spectrometer were optimized, brain smears were analyzed for 1.15 min moving the spray across the slide in a serpentine pattern to avoid spatial bias. The isolation window was set to 3 m/*z* to allow simultaneous isolation and fragmentation of 2HG (*m/z* 147) and glutamate (Glu, *m/z* 146), the latter serving as an endogenous reference molecule. 2HG and Glu undergo water loss during CID and forming fragment ions at *m/z* 129 and 128, respectively. In MRM experiments, ionization by DESI using 0.80 kV with MeOH flowing at 3 μL min^{-1} as the solvent and better than unit mass resolution was employed. Two MRM transitions were recorded iteratively: the first quadrupole isolated 2HG (*m/z* 147) and Glu (*m/z* 146) simultaneously, while the third quadruple scanned a narrow mass range to record the intensities of dehydrated 2HG (m/z 129) and Glu (m/z 128). The MRM experiments were done as the stage moved down the slide in parallel lines over a total period of 100 s. Each smear was analyzed three times. See section S2 for more details on the selection of targeted biomarkers.

Data analysis

Two customized MATLAB algorithms were written for data filtration and processing; as the LIT produces data in a spectral format (product ion spectra) and the TQ produces total ion current (TIC) for each channel.

IDH mutation scores for both measurements were calculated using the same approach as reported in previous studies[10,22]. Since 2HG and Glu fragments are one mass unit apart, the isotopic contribution of ^{13}C-Glu to m/z 129 was first subtracted and then the ratio of 129 to 128 was calculated (Eq. 1).

$$IDHmutationscore = \frac{I_{129} - (I_{128} \times 0.061)}{I_{128}} \quad (1)$$

The average IDH mutation scores of the three experiments were calculated for statistical analysis. Table S4 shows a representative IDH mutation score data set obtained by DESI-LIT and DESI-TQ.

MetaboAnalyst 6.0 was used to obtain the receiver operating characteristic (ROC) curve, area under the curve (AUC), and the cutoff value for the IDH mutation score. At the optimal cutoff, the sensitivity, specificity, and accuracy of DESI predictions were calculated from the confusion matrix. A two-sample Wilcoxon rank-sum (Mann–Whitney) test was performed using STATA with $p < 0.05$ taken as being significant.

Data availability

The datasets analyzed during the current study are available in the Purdue University Research Repository (PURR), https://purr.purdue.edu/publications/4545/1.

Received: 22 July 2024; Accepted: 18 October 2024
Published online: 06 November 2024

References

1. Louis, D. N. et al. The 2021 WHO classification of tumors of the central nervous system: A summary. *Neuro Oncol.* **23**, 1231–1251 (2021).
2. Louis, D. N. et al. The 2021 WHO classification of tumors of the central nervous system: A summary. *Neuro Oncol.* **23**, 1231–1251 (2016).
3. Brem, S. & Abdullah, K. G. *Glioblastoma* (Elsevier Health Sciences, 2016).
4. Pianka, S. T. et al. D-2-HG inhibits IDH1mut glioma growth via FTO inhibition and resultant m6A hypermethylation. *Cancer Res. Commun.* **4**, 876–894 (2024).
5. Attenello, F. J. et al. Use of gliadel (BCNU) wafer in the surgical treatment of malignant glioma: A 10-year institutional experience. *Ann. Surg. Oncol.* **15**, 2887–2893 (2008).
6. Shah, S. R. et al. Verteporfin-loaded polymeric microparticles for intratumoral treatment of brain cancer. *Mol. Pharm.* **16**, 1433–1443 (2019).
7. Schiapparelli, P. et al. Self-assembling and self-formulating prodrug hydrogelator extends survival in a glioblastoma resection and recurrence model. *J. Controll. Release* **319**, 311–321 (2020).
8. Han, P. et al. IDH mutation in glioma: molecular mechanisms and potential therapeutic targets. *British J Cancer* **122**(11), 1580–1589. https://doi.org/10.1038/s41416-020-0814-x (2020).
9. Leather, T., Jenkinson, M., Das, K. & Poptani, H. Magnetic resonance spectroscopy for detection of 2-hydroxyglutarate as a biomarker for IDH mutation in gliomas. *Metabolites* **7**(2), 29. https://doi.org/10.3390/metabo7020029 (2017).
10. Brown, H. M. et al. Intraoperative detection of isocitrate dehydrogenase mutations in human gliomas using a miniature mass spectrometer. *Anal Bioanal Chem* **411**, 7929–7933 (2019).
11. Brown, H. M. et al. Intraoperative mass spectrometry platform for IDH mutation status prediction, glioma diagnosis, and estimation of tumor cell infiltration. *J. Appl. Lab. Med.* **6**, 902–916 (2021).
12. Cancer Genome Atlas Research Network. Comprehensive, integrative genomic analysis of diffuse lower-grade gliomas. *New England J Med* **372**(26), 2481–2498. https://doi.org/10.1056/NEJMoa1402121 (2015).
13. Zulkarnain, S., Yunus, N., Kandasamy, R., Zun, A. B. & Zin, A. A. M. Evaluation study of intraoperative cytology smear and frozen section of glioma. *Asian Pac J Cancer Prev* **21**, 3085 (2020).
14. Zin, A. A. M. & Zulkarnain, S. Diagnostic accuracy of cytology smear and frozen section in glioma. *Asian Pac J Cancer Prev* **20**, 321 (2019).
15. Chakrabarty, S., LaMontagne, P., Shimony, J., Marcus, D. S. & Sotiras, A. MRI-based classification of IDH mutation and 1p/19q codeletion status of gliomas using a 2.5D hybrid multi-task convolutional neural network. *Neuro-Oncol. Adv.* **5**(1), vdad023. https://doi.org/10.1093/noajnl/vdad023 (2023).
16. Chen, R. et al. Molecular features assisting in diagnosis, surgery, and treatment decision making in low-grade gliomas. *Neurosurg. Focus FOC* **38**, E2 (2015).
17. Gerard, I. J. et al. Brain shift in neuronavigation of brain tumors: A review. *Med Image Anal* **35**, 403–420 (2017).
18. Sobottka, S. B., Geiger, K. D., Salzer, R., Schackert, G. & Krafft, C. Suitability of infrared spectroscopic imaging as an intraoperative tool in cerebral glioma surgery. *Anal. Bioanal. Chem.* **393**, 187–195 (2009).
19. Brusatori, M. et al. Intraoperative raman spectroscopy. *Neurosurg. Clin. N. Am.* **28**, 633–652 (2017).
20. Wang, N. et al. Deep learning-based optical coherence tomography image analysis of human brain cancer. *Biomed. Opt. Express* **14**, 81 (2023).
21. King, M. E. et al. Rapid diagnosis and tumor margin assessment during pancreatic cancer surgery with the MasSpec Pen technology. *Proc. Nat. Acad. Sci.* **118**, e2104411118 (2021).
22. Hua, W. et al. Rapid detection of IDH mutations in gliomas by intraoperative mass spectrometry. *Proc. Nat. Acad. Sci.* **121**(23), e2318843121. https://doi.org/10.1073/pnas.2318843121 (2024).
23. Davis, D. E. Jr., Sherrod, S. D., Gant-Branum, R. L., Colby, J. M. & McLean, J. A. Targeted strategy to analyze antiepileptic drugs in human serum by LC-MS/MS and LC-Ion mobility-MS. *Anal. Chem.* **92**, 14648–14656 (2020).
24. Pekov, S. I. et al. Mass spectrometry for neurosurgery: Intraoperative support in decision-making. *Mass Spectrom. Rev.* https://doi.org/10.1002/mas.21883 (2024).
25. Takats, Z., Strittmatter, N. & McKenzie, J. S. Ambient Mass Spectrometry in Cancer Research. In *Applications of Mass Spectrometry Imaging to Cancer* 231–256 (Elsevier, 2017). https://doi.org/10.1016/bs.acr.2016.11.011.
26. Keating, M. F. et al. Data acquisition and intraoperative tissue analysis on a mobile, battery-operated. *Orbitrap Mass Spectrometer. Anal Chem* https://doi.org/10.1021/acs.analchem.4c00722 (2024).
27. Woolman, M. et al. Lipidomic-based approach to 10 s classification of major pediatric brain cancer types with picosecond infrared laser mass spectrometry. *Anal. Chem.* **96**, 1019–1028 (2024).
28. Zirem, Y. et al. Real-time glioblastoma tumor microenvironment assessment by SpiderMass for improved patient management. *Cell Reports Med.* **5**(4), 101482. https://doi.org/10.1016/j.xcrm.2024.101482 (2024).

29. Morato, N. M. & Cooks, R. G. Desorption electrospray ionization mass spectrometry: 20 years. *Acc Chem Res* **56**, 2526–2536 (2023).
30. Takáts, Z., Wiseman, J. M., Gologan, B. & Graham Cooks, R. *Mass Spectrometry Sampling Under Ambient Conditions with Desorption Electrospray Ionization*. *Ind. Eng. Chem. Process Des. Dev* vol. 297 www.sciencemag.org/cgi/content/full/306/5695/469/www.sciencemag.orgSCIENCEVOL30615OCTOBER2004 (1998).
31. Awad, D. et al. Adipose triglyceride lipase is a therapeutic target in advanced prostate cancer that promotes metabolic plasticity. *Cancer Res.* **84**, 703–724 (2024).
32. Chen, R., Brown, H. M. & Cooks, R. G. Metabolic profiles of human brain parenchyma and glioma for rapid tissue diagnosis by targeted desorption electrospray ionization mass spectrometry. *Anal. Bioanal. Chem.* **413**(25), 6213–6224 (2021).
33. Morato, N. M. et al. High-throughput analysis of tissue microarrays using automated desorption electrospray ionization mass spectrometry. *Sci. Rep.* **12**(1), 18851. https://doi.org/10.1038/s41598-022-22924-4 (2022).
34. Weigand, M. R. et al. Lipid isobar and isomer imaging using nanospray desorption electrospray ionization combined with triple quadrupole mass spectrometry. *Anal Chem* https://doi.org/10.1021/acs.analchem.3c04705 (2023).
35. Snyder, D. T., Szalwinski, L. J., Wells, J. M. & Cooks, R. G. Logical MS/MS scans: A new set of operations for tandem mass spectrometry. *Analyst* **143**, 5438–5452 (2018).
36. Cordeiro, F. B. et al. Multiple reaction monitoring (MRM)-profiling for biomarker discovery applied to human polycystic ovarian syndrome. *Rapid Commun. Mass Spectromet.* **31**, 1462–1470 (2017).
37. Marasco, C. A. et al. Suspect screening of exogenous compounds using multiple reaction screening (MRM) profiling in human urine samples. *J. Chromatogr. B* **1201–1202**, 123290. https://doi.org/10.1016/j.jchromb.2022.123290 (2022).
38. Pu, F. et al. Rapid determination of isocitrate dehydrogenase mutation status of human gliomas by extraction nanoelectrospray using a miniature mass spectrometer. *Anal. Bioanal. Chem.* **411**, 1503–1508 (2019).
39. Alfaro, C. M. et al. Intraoperative assessment of isocitrate dehydrogenase mutation status in human gliomas using desorption electrospray ionization–mass spectrometry. *J. Neurosurg. JNS* **132**, 180–187 (2020).
40. Quiñones-Hinojosa A, et al. (2024) From the operating room to the laboratory: role of the neuroscience tissue biorepository in the clinical, translational, and basic science research pipeline. In: Mayo Clinic Proceedings (Vol. 99, No. 2, pp. 229-240). Elsevier.
41. Pirro, V. et al. Utility of neurological smears for intrasurgical brain cancer diagnostics and tumour cell percentage by DESI-MS. *Analyst* **142**, 449–454 (2017).

Acknowledgements

The authors thank Kenneth Virgin for his contribution to data processing. This work was supported by the Innovative Molecular Analysis Technologies (IMAT) Program of the National Cancer Institute of the NIH (R33CA240181-01A1), Waters Corporation (Grant Number 40002775), and the Purdue University Institute for Cancer Research (NIH grant P30 CA 023168). A.Q.-H. acknowledges the support from Richard and Lauralee Uihlein, the William J. and Charles H. Mayo Professorship, the Mayo Clinic Clinician Investigator Award, the Florida Department of Health Cancer Research Chair Fund, the Monica Flynn Jacoby Endowed Chair, BPJK Cleveland Family Foundation Neurosurgery Biobank and Registry Fund, and the Jacquie Lorraine Goldman Fund for a Brain Tissue Bank.

Statement on diagnostic use

The instrumentation used in this study is not intended for diagnostic use.

Author contributions

R.G.C. designed the experiments with contributions from A.Q.-H. and M.M. and M.S. performed experiments and analyzed data. R.G.C. and M.S. wrote the initial draft of the manuscript. A.Q.-H. and D.M. provided tissues and expertise and contributed to study design and writing. S.P. and M.M. prepared Waters prototype DESI and TQ instrument and contributed to study design. All authors critically reviewed the manuscript.

Funding

The Funding was provided by IMAT NIH, (R33CA240181), (R33CA240181), (R33CA240181), (R33CA240181), Purdue University Center for Cancer Research, P30 CA 023168, P30 CA 023168,Waters Corporation, 40002775, 40002775

Declarations

Competing interests

The authors declare no competing interests.

Additional information

Supplementary Information The online version contains supplementary material available at https://doi.org/10.1038/s41598-024-77044-y.

Correspondence and requests for materials should be addressed to R.G.C.

Reprints and permissions information is available at www.nature.com/reprints.

Publisher's note Springer Nature remains neutral with regard to jurisdictional claims in published maps and institutional affiliations.

Open Access This article is licensed under a Creative Commons Attribution-NonCommercial-NoDerivatives 4.0 International License, which permits any non-commercial use, sharing, distribution and reproduction in any medium or format, as long as you give appropriate credit to the original author(s) and the source, provide a link to the Creative Commons licence, and indicate if you modified the licensed material. You do not have permission under this licence to share adapted material derived from this article or parts of it. The images or other third party material in this article are included in the article's Creative Commons licence, unless indicated otherwise in a credit line to the material. If material is not included in the article's Creative Commons licence and your intended use is not permitted by statutory regulation or exceeds the permitted use, you will need to obtain permission directly from the copyright holder. To view a copy of this licence, visit http://creativecommons.org/licenses/by-nc-nd/4.0/.

© The Author(s) 2024